Int J Clin Exp Pathol 2017;10(6):7125-7134
www.ijcep.com /ISSN:1936-2625/IJCEP0047507

Original Article

miR-21 targets MMP-7 and promotes perineural invasion of cholangiocarcinoma

Xiaochun Zhao, Jing Li, Qiang Shen, Bin Yu

Department of Imaging Center, The Affiliated Hospital of Jining Medical College, Jining, China

Received December 27, 2016; Accepted March 4, 2017; Epub June 1, 2017; Published June 15, 2017

Abstract: Objective: Perineural invasion (PNI) is a form of cholangiocarcinoma (CC) metastasis. This behavior is associated with poor clinical outcomes. Therefore, it is critical to identify novel interactions between nerves and cancer cells that support the process of PNI. Precious study has found that upregulated miR-21 and MMPs could increase tumor metastasis and invasion by its various targets in many cancer cells. In the present study, we assessed whether miR-21 promoted invasion and PNI of CC cells and explored its mechanisms. Methods: miR-21 was transfected into the CCLP1 cells to construct stable miR-21 transfected clones (miR-21/CCLP1). The miR-21/CCLP1 cells were transiently transfected into MMP-7 siRNA. Cell invasion and migration were detected by transwell migration assays and wound healing assay. Dorsal root ganglion (DRG) and miR-21/CCLP1 or miR-21/MMP-7 siRNA/CCLP1 cells were co-cultured for 7 days to construct in vitro coculture model of nerve invasion. miR-21/CCLP1 and scramble/CCLP1 cells (2×10^5) in 3 μl volume of PBS were microscopically injected into the distal sciatic nerve, under the epineurium to construct in vivo model of sciatic nerve invasion. Murine sciatic nerve tumors generated from miR-21/CCLP1 and scramble/CCLP1 cells were assessed by magnetic resonance imaging (MRI). miR-21 expression was detected by quantitative reverse transcriptase polymerase chain reaction (qRT-PCR); MMP-7 was detected by western blot assay. Results: miR-21 overexpression promoted invasion and migration in vitro by upregulation of MMP-7. In vitro nerve and cancer co-culture invasion assays of PNI demonstrated that cancer cell miR-21 expression facilitates PNI by upregulation of MMP-7. Sciatic nerve tumors generated from miR-21/CCLP1 cells grew more rapidly than those generated from scramble/CCLP1 tumors at week 6. Clinical evaluation at the time of surgical exploration confirmed the MRI findings, demonstrating thickened and infiltrated proximal sciatic nerves for the miR-21/CCLP1 tumors, as compared with normal appearing proximal sciatic nerves in non-tumor bearing animals. Conclusions: miR-21 promotes CC invasion, migration and PNI though MMP-7-mediated signaling.

Keywords: Cholangiocarcinoma, perineural invasion, miR-21, MMP-7

Introduction

Cholangiocarcinoma (CC) is divided into three general categories: intrahepatic, hilar or distal. Although hilar CC remains the most common type, the incidence of intrahepatic cholangiocarcinoma (IHCC) is rising and IHCC currently accounts for 20% of all CC [1]. Due to its difficulty of diagnosis, vascular invasion, perineural invasion, intrahepatic metastasis, perihepatic lymph node metastasis and post-resection recurrence, the five-year survival rate is only 5%, and this survival rate had not vastly improved in past three decades [2].

CC via perineural invasion (PNI) is an extremely part during its genesis and development especially the early period. PNI is highly correlated with tumor volume, location, depth of invasiveness, angiogenesis and lymph node involvement [1]. While the tumor perineural invasion is generated in cholangiocarcinoma, it indicated that the tumor is not only localized in the primary organ, but metastasis in distance or the tumor cell residue stays in abdominal cavity, the proportion of perineural invasion in CC is around 85-88%. Furthermore, it is quite hard to radical cure by the operation and the clinical prognosis is extremely bad [3].

PNI is actually a type of tumor local growth pattern. The perineural interspace invasion was the fifth dependent metastasis pathway to be discovered. In PNI, leap metastasis is possible,

CC could metastasize into liver via the neural interspace [4]. However, the possible mechanisms of PNI in CC are not very clear. Understanding the possible mechanisms, and searcing for novel methods and targets to prevent perineural invasion in early-phase CC is the direction of effort.

miR-21 was one of the most frequently studied cancer-related miRNAs and dysregulated in most cancers by acting as oncogene [5]. Upregulated miR-21 could increase tumor growth, metastasis and invasion and reduce sensitivity to chemotherapy by its various targets [6]. Cancer patients with higher expression of miR-21 always had a worse prognostic outcome. In cholangiocarcinoma cells, over-expression of miR-21 significantly promoted cell migration, invasion and xenografts growth, whereas contrary phenomenon was observed in mir-21 inhibitor group [7]. In addition, miR-21 was found to be higher expressed in PNI tumors than non-PNI tumors [8].

Increased expression and activity of various matrix metalloproteinases (MMPs), most notably MMP-7 and -9, are associated with tumor invasion and metastasis in malignant neoplasms, including intrahepatic cholangiocarcinoma [9-11]. Unlike MMP-9, which is expressed in both the carcinoma and tumor stromal cells of intrahepatic cholangiocarcinoma, MMP-7 is mainly expressed in malignant cholangiocytes [11], suggesting its intrinsic value as a hepatobiliary tumor cell marker. MMP-7 was also seen to be more frequently expressed in invasive non-papillary cholangiocarcinomas than in the papillary type showing a lesser depth of tumor invasion and infrequent metastasis [11]. Other study has reported that high MMP-7 expression seems to correlate with tumor lymphatic metastasis, PNI, higher malignancy and less favorable prognosis in CC patients [9].

Martin et al. has reported that increased expression of miR-21 enhanced the invasive potential of melanoma cell lines through TIMP3 inhibition [12]. Liu et al. has reported that miR-21 induces tumor angiogenesis through targeting PTEN, leading to activate AKT and ERK1/2 signaling pathways, and thereby enhancing HIF-1α and VEGF expression [13]. In laryngeal squamous cell carcinoma (LSCC), miR-21 is involved in the cell migration and tumorigenicity via the regulation of MMP-2 expression [14]. Similarly, MMP-7 expression was inhibited by miR-21 in glioma although the molecular mechanisms remain unclear [15].

In the present study, we use miR-21 overexpressing CC cells to determine if miR-21 can promote migration and invasion of CC cells in vitro. We use DRG as part of an *in vitro* co-culture assay with CC cells as a model of PNI. We used in vivo model of sciatic nerve invasion to study the role of miR-21 on PNI. In this study, we identified a new role of miR-21 in PNI and revealed the underlying mechanisms. These results indicated that miR-21 promotes invasion and PNI via activation of MMP-7 signals.

Materials and methods

Cell culture

Human cholangiocarcinoma (CCA) cell lines, HuCCT1, CCLP1, TFK1 and noncancerous cholangiocyte cell line (H69) were purchased from Gibco Invitrogen (Auckland, New Zealand). The H69 cells were cultured in Bronchial Epithelial Cell Basal Medium (Lonza, Walkersville, MD) with supplemental growth factors in BEGM SingleQuot Kit and 10% heat-inactivated FBS. Other cells were cultured in RPMI-1640 medium containing 10% FBS were cultured at 37°C in a humidified atmosphere containing 5% CO_2.

Stable transfection

miR-21 expression and scramble control lentivirus particles with enhanced green flurescent protein (eGFP) were purchased from GeneCopoeia (Rockville, MD). The CCLP1 cells were transduced with miR-21 expressing lentiviral particles or scramble control overnight. After 72 hr, the medium was replaced with fresh medium containing puromycin for selection and the subsequent cultures were continued in the presence of 1 μg/ml puromycin. After the cells reached confluence, total RNA was extracted and quantitative reverse transcription polymerase chain reaction (qRT-PCR) was performed to verify the levels of miR-21.

siRNA transfection

(miR-21/CCLP1 and scramble/CCLP1) cells (2×10^5 cells per well) were plated in 6-well plates and allowed to grow overnight. 2 nM MMP-7 siRNA or scramble siRNA and 5 μl

Lipofectamine™ 2000 (Invitrogen, Carlsbad, CA) were diluted in OPTI-MEM (Invitrogen, Carlsbad, CA) to a total volume of 250 μl. The diluted siRNA and Lipofectamine™ 2000 were mixed and incubated at ambient temperature for 20 minutes. The cells were washed with serum-free DMEM medium, and then the diluted siRNA mix was added to the 6-well plates for 6 hours, after which the mix was replaced with growth medium and cultured for another 48 h.

Western blot

Total protein extracts were separated by 10-12% SDS-PAGE, and electro-transferred to polyvinylidene fluoride membranes. Anti-MMP-7 (1:200, Cell Signaling Technology) and anti-β-actin (1:1000, Abcam, Cambridge, UK) antibodies were diluted in PBS/T (PBS/tween; 5% milk powder) and incubated with the membranes at 4°C overnight. The appropriate secondary antibody was applied (1:2000, horseradish peroxidase-conjugated anti-mouse and anti-rabbit) at room temperature for 1 h. Immunoreactive proteins were visualised by enhanced chemiluminescence (Amersham Bioscience, Hangzhou, China).

MMP-7 expression measured by ELISA

The amount of MMP-9 secreted into the cell culture supernatant was measured with an ELISA kit (Guangzhou, China) as the manufacture's instruction. The optical density at 450 nm was measured with a plate reader.

RNA extraction and quantitative real-time PCR (qRT-PCR)

Total miRNA was isolated using the *mir*Vana miRNA isolation kit (Ambion). miRNA was extended by a poly(A) tailing reaction using the A-Plus poly(A) polymerase tailing kit (Cell Script). cDNA was synthesized from miRNA with poly(A) tail using a poly(T) adaptor primer and qScript™ reverse transcriptase (Quanta Biogenesis). The expression level of *miR-21* was quantified with the SYBR Green qRT-PCR kit (Ambion) using an miRNA-specific forward primer and a universal poly(T) adaptor reverse primer. The expression of *miR-21* was defined based on the threshold (*Ct*), and the relative expression levels were calculated as $2^{-[(Ct \text{ of } miR\text{-}21) - (Ct \text{ of } U6)]}$ after normalization with reference to the expression of U6 small nuclear RNA.

Matrigel invasion assay

The Boyden chamber technique (transwell analysis) was performed. Briefly, the 8-μm pore size filters were coated with 100 μl of 1 mg/ml matrigel (dissolved in serum-free RPMI1640 medium). 600 μl of RPMI1640 medium containing 10% FBS was added to the lower chambers. Forty-eight hrs post-transfection, homogeneous single cell suspensions (1×10^5 cells/well) were added to the upper chambers and allowed to invade for 24 hrs at 37°C in a CO_2 incubator. Cells remaining attached to the upper surface of the filters were carefully removed with cotton swabs. Migrated cells were stained with 0.1% crystal violet for 10 min at room temperature and examined by light microscopy. Quantification of migrated cells was performed according to the manufacturer's instruction.

Wound healing assay

Cells were seeded into 6-well plates and cultured in standard media until confluence. The media was discarded and a wound was simulated by creating scratches across the plate using a 200-μl pipette tip. The plates were washed twice with serum-free media and the cells observed and photographed using microscopy to ensure that there were sufficient cells t the leading edge of the wound. The cells were then grown in serum-free medium for 24 hrs before final images were acquired. Migration rates were calculated by measuring the distance traveled toward the center of the wound.

In vitro coculture model of nerve invasion

Harvested DRG were each implanted in the center of a 15-μL drop of growth factor-depleted Matrigel in a six-well plate with glass bottom. At day 7 after DRG implantation, miR-21/CCLP1, scramble/CCLP1 and miR-21/MMP-7 siRNA CCLP1 (5×10^4) cells were added to the media around the DRG. 6 d after the cells were added, plates were examined on an Axiovert 200 M microscope (Carl Zeiss), and images were acquired using a Photometrics Coolsnap ES camera (Photometrics). Software (MetaMorph 7.7.4; Molecular Devices) was used to outline and quantify the areas within the DRG invaded by cancer cells.

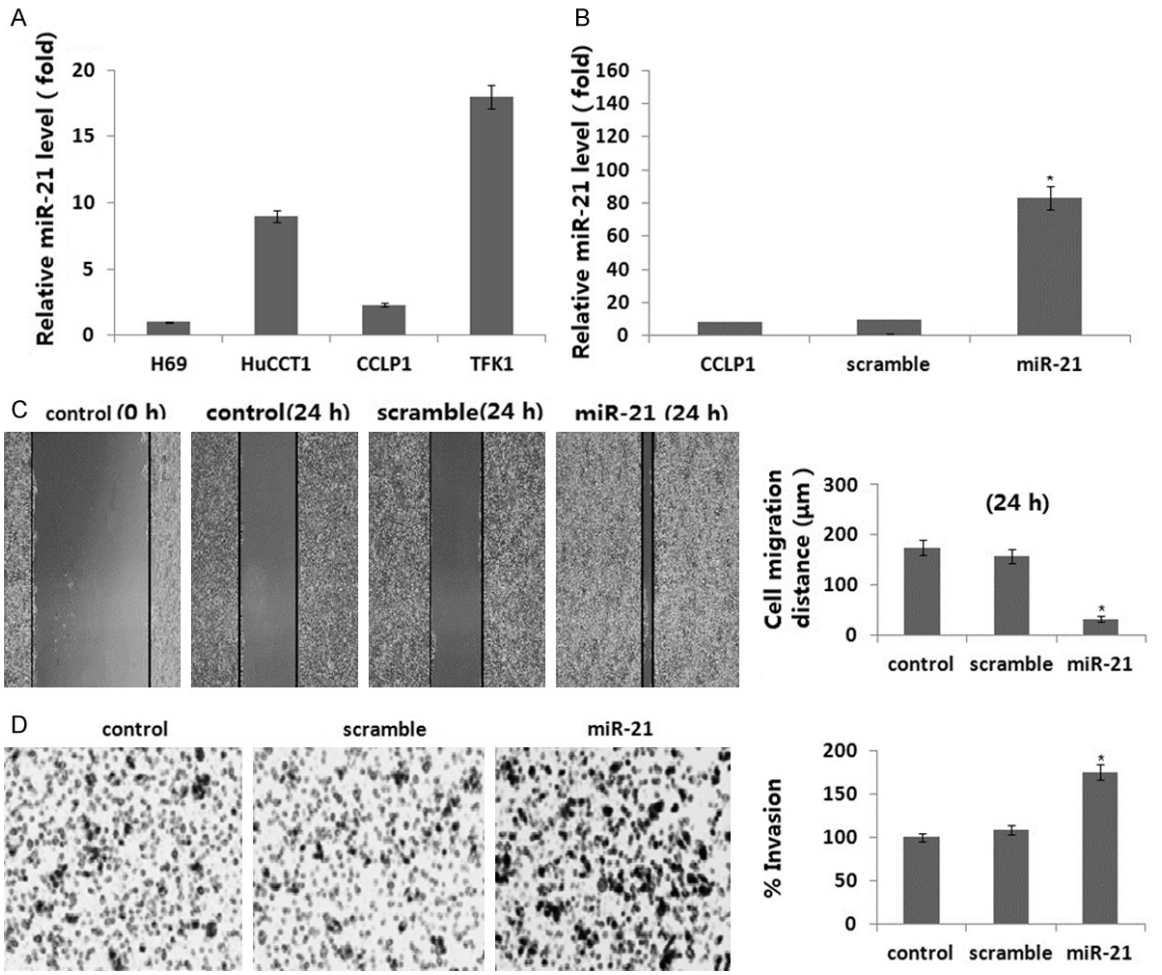

Figure 1. miR-21 promoted cell migration and invasion in CCLP1 cells. A. miR-21 level was measured by real-time RT-PCR in HuCCT1, CCLP1, TFK1 and H69 cells. B. miR-21 levels was detected in the stable miR-21 and scramble control lentivirus particles transfected CCLP1 cells; C. The cell motility was detected using wound healing assay in CCLP1 cells transfected with miR-21. D. The cell invasion was detected Transwell chambers assay. $^{*}P<0.01$, vs control.

In vivo model of sciatic nerve invasion

Nude athymic mice were anesthetized with isoflurane and their right sciatic nerves were surgically exposed. Ten mice were distributed randomly into two groups. miR-21/CCLP1 and scramble/CCLP1 cells (2×10^5) in 3 μl volume of PBS were microscopically injected into the distal sciatic nerve, under the epineurium, using a 10-μl Hamilton syringe. Additional mice underwent sciatic nerve injection with PBS as non-tumor bearing controls. The sciatic nerve innervates the hind limb paw muscles. Sciatic nerve function was measured using the following the (a) *sciatic neurological score*, which grades hind limb paw response to manual extension of the body, from 4 (normal) to 1 (total paw paralysis); and (b) *sciatic nerve function index*, which measures the spread width between the first and fifth toes of the hind limbs. These measures were normal in all mice immediately after surgical implantation of the cancer cells.

MRI assessment of in vivo perineural invasion

Murine sciatic nerve tumors generated from miR-21/CCLP1 and scramble/CCLP1 cells were assessed by magnetic resonance imaging (MRI). After the mice were anesthetized with isoflurane, sciatic nerves were localized by a scout fast spin echo scan in three orientations, followed by a coronal T2-weighted fast spin-echo image. Images were used to visually assess the caliber of the sciatic nerve as it courses proximal to the primary tumor injection site. Sciatic nerve invasion length based

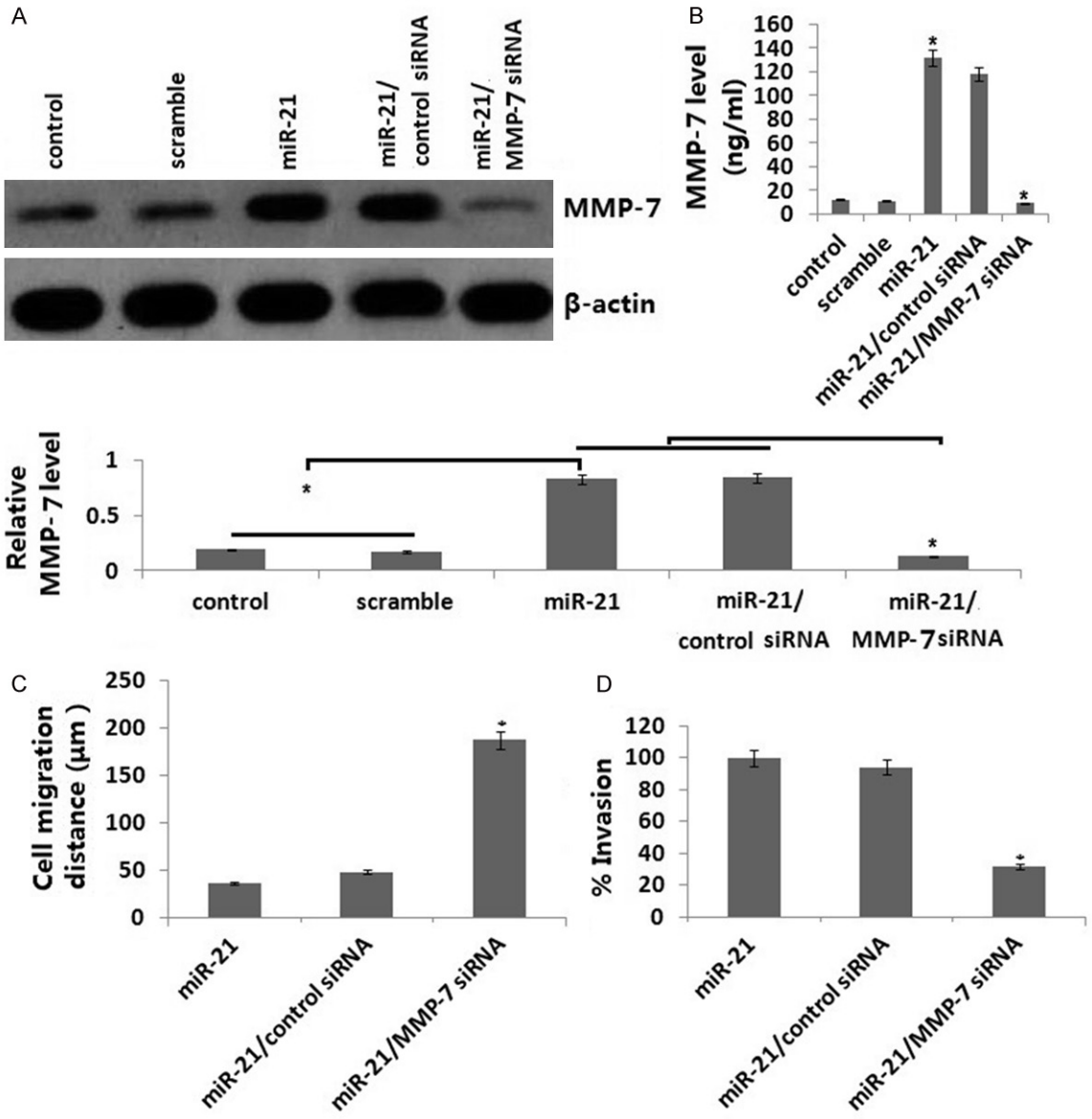

Figure 2. miR-21 facilitates invasion and migration of CCLP1 cells by activating MMP-7 in vitro. A. MMP-7 expression was detected by western blot assay; B. MMP-7 level was detected by ELISA assay; C. The cell motility was detected using wound healing assay in CCLP1 cells transfected with miR-21/MMP-7 siRNA. D. The cell invasion was detected Transwell chambers assay. *P<0.01, vs control.

on MRI imaging was assessed. Images showing a thickened sciatic nerve were analyzed with Image J.

Immunohistochemistry

All tumors was fixed in 10% buffered formalin (Biochemical Science Inc, Shanghai, China). Tissue sections were cut at (4 μm). Following incubation with the MMP-7 primary antibody, sections were thoroughly rinsed in wash buffer and subsequently incubated in peroxidase coupled secondary antibody (30 min). After, sections were washed in buffer and immunodetection was performed by treatment with the chromogenic 3-3 diaminobenzidine (DAB) solution. Finally sections were counterstained with hematoxylin, dehydrated by submerging in a series of ethanol, fixed in xylene, mounted and coverslipped.

Statistical analyses

A Student t test was used for statistical analysis as appropriate. All *P* values were calculated using two-sided tests. Differences were consid-

ered statistically significant if the *P* value was less than 0.05. Error bars in the graphs represent 95% confidence intervals.

Results

MiR-21 inhibits migration and invasion of CCLP1 cells in vitro

miR-21 expression was detected in human cholangiocarcinoma (CCA) cell lines, HuCCT1, CCLP1, TFK1 and noncancerous cholangiocyte cell line (H69) by qRT-PCR. The lest miR-21 expression was shown in the CCLP1 cells (**Figure 1A**). So we used CCLP1 cells for further study.

miR-21 was stably transfected into CCLP1 cells. The level of miR-21 was detected using qRT-PCR in miR-21 transfected cells. The results showed that miR-21 expression increased 59 fold compared to the untreated or scramble transfected CCLP1 cells (**Figure 1B**).

Next, we measured the cell motility and invasion capacities in CCLP1 cells transfected with miR-21. The wound healing assay showed that miR-21 promoted the cell motility in CCLP1 cells (**Figure 1C**). Consistent with this, overexpression of miR-21 enhanced the invasion in CCLP1 cells (**Figure 1D**). Taken together, our findings miR-21 is involved in promoting cell migration and invasion in CCLP1 cells.

miR-21 facilitates CCLP1 invasion and migration by activating MMP-7 in vitro

To investigate the potential mechanism of miR-21 on invasion and migration of CCLP1 cells, we examined the MMP-7 expression in CCLP1 cells and supernatant by western blot and ELISA assay. We show that the MMP-7 was significantly increased in miR-21 stably transfected CCLP1 cells (miR-21/CCLP1) compared to the scramble transfected cells and untreated cells (**Figure 2A**, **2B**). Targeting MMP-7 by siRNA in the miR-21/CCLP1 cells significantly inhibited MMP-7 expression in the miR-21/CCLP1 cells by western blot and ELISA assay (**Figure 2A**, **2B**). The wound healing assay showed that targeting MMP-7 by siRNA inhibited cell motility and invasion in the miR-21/CCLP1 cells (**Figure 2C**, **2D**), suggesting that miR-21 facilitates CCLP1 invasion and migration by activating MMP-7.

miR-21 facilitates perineural invasion by activating MMP-7 in vitro

We performed DRG co-culture assays to assess for PNI *in vitro.* DRG harvested from miR-21/CCLP1 cells exhibit progressive cancer cell invasion along DRG neuritis in the 6th days compared to the scramble/CCLP1 harvested DRG (**Figure 3**). However, DRG harvested from miR-21/MMP-7 siRNA/CCLP1 cells demonstrate diminished invasion along DRG neurites in the 6th days (**Figure 3**). Furthermore, the area of nerve invasion was significantly reduced in the miR-21/MMP-7 siRNA groups compared with the miR-21 groups and scramble groups (**Figure 3**). These results demonstrate that miR-21 facilitates perineural invasion by activating MMP-7 in vitro.

MiR-21 expression facilitates prostate cancer perineural in vivo

We next assessed the contribution of CCLP1 expression in PNI using a murine *in vivo* model of sciatic nerve invasion. Sciatic nerve tumors generated from miR-21/CCLP1 cells grew more rapidly than those generated from scramble/CCLP1 cells, and untreated tumors at week 5. MRI imaging of miR-21 tumors showed thickened sciatic nerves at week 5 extending proximal to the primary tumors towards the spinal cord, consistent with PNI (**Figure 4A**). In contrast, MRI imaging of control tumors showed preservation of thin proximal sciatic nerves at week 5 (**Figure 2A**), similar to those of normal mice lacking any tumor (**Figure 4A**). Clinical evaluation at the time of surgical exploration confirmed the MRI findings, demonstrating thickened and infiltrated proximal sciatic nerves for the miR-21 tumors at week 5 (**Figure 4B**), as compared with normal sciatic nerves in non-tumor bearing animals (**Figure 4B**). Our immunohistochemistry analysis showed that miR-21 significantly upregulated MMP-7 expression within tumors (**Figure 4C**).

Discussion

PNI is an ominous clinical problem where cancer cells are found to track and invade along nerves, often extending toward the central nervous system, which permitting unpredictable cancer progression beyond the expected anatomic extent of a tumor mass, making complete surgical resection more difficult and requiring

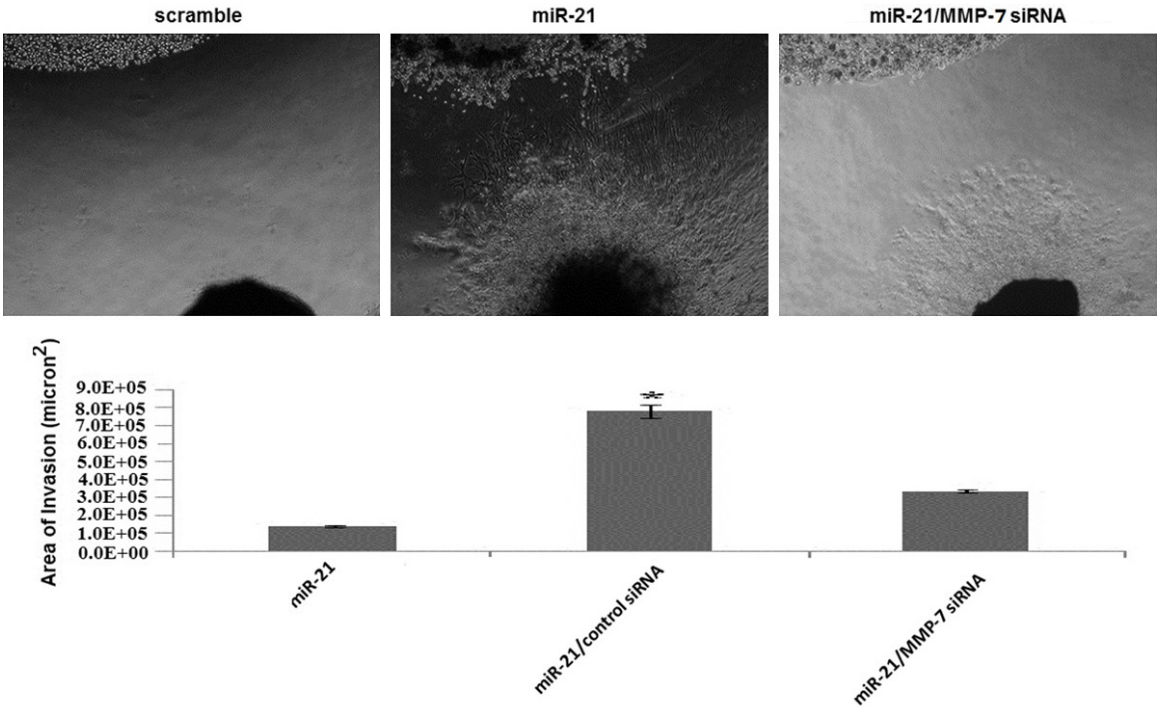

Figure 3. miR-21 facilitates perineural invasion by activating MMP-7 in vitro. Dorsal root ganglia (DRG) and cancer co-culture assay of PNI permits the assessment of interactions between cancer and nerve cells. Coculture of murine DRG with miR-21/CCLP1, scramble/CCLP1 and miR-21/MMP-7 siRNA/CCLP1 cells in Matrigel permits assessment of the degree of PNI by day 6. The mean total area of invasion is compared between three groups ($P<0.05$; t test).

large radiation fields designed to cover the affected nerves [16]. PNI may also cause significant morbidity, inducing paralysis, pain, or paresthesias of the affected nerves [17]. PNI has been implicated as a poor prognostic factor in many cancer types, including squamous cell carcinoma of the head and neck, cancer of the prostate, and colorectal and pancreatic cancers [18-22]. In a large series of hilar and intrahepatic CC, Endo and colleagues showed that the presence of PNI was significantly associated with reduced OS [23]. Fisher et al. have demonstrated that the presence of PNI was found to be significantly associated with a worse prognosis, even after accounting for other known adverse factors, such as large tumour size, multiple tumours, positive resection margin, poor differentiation and LN involvement [24]. However, the precise molecular mechanisms underlying PNI remain unclear. Most current theories suggest that reciprocal signaling and interactions occur between cancer cells and the nerve microenvironment induce this event [17, 25].

Sousa et al. [26] has recently reported that presence of PNI was associated with low miR-199b levels. In addition, miR-21 levels were high whereas miR-100 and miR-125b levels were low in HNSCC compared to the resection margins. The increase of miR-21 and the reduction of PTEN levels contribute to cancer growth and spread. Prueitt et al. has reported that nineteen microRNAs were found to be higher expressed in PNI tumors than non-PNI tumors [27]. Furthermore, *miR-21* and *miR-224* are located in malignancy-associated chromosomal regions that were found to have an increased gene expression in human prostate cancer [8]. From the studies above, we suggested that overexpression of miR-21 contributed to cancer invasion.

In the present study, the expression of miR-21 in several CC cell lines was determined using qRT-PCR. miR-21 expression was significantly increased in all 3 CC cell lines compared with normal cholangiocyte cell line (H69). We subsequently found that overexpression of miR-21 significantly suppressed CC cell invasion and migration in vitro.

We next hypothesized that miR-21 signaling may play a role in CC PNI. To identify miR-21

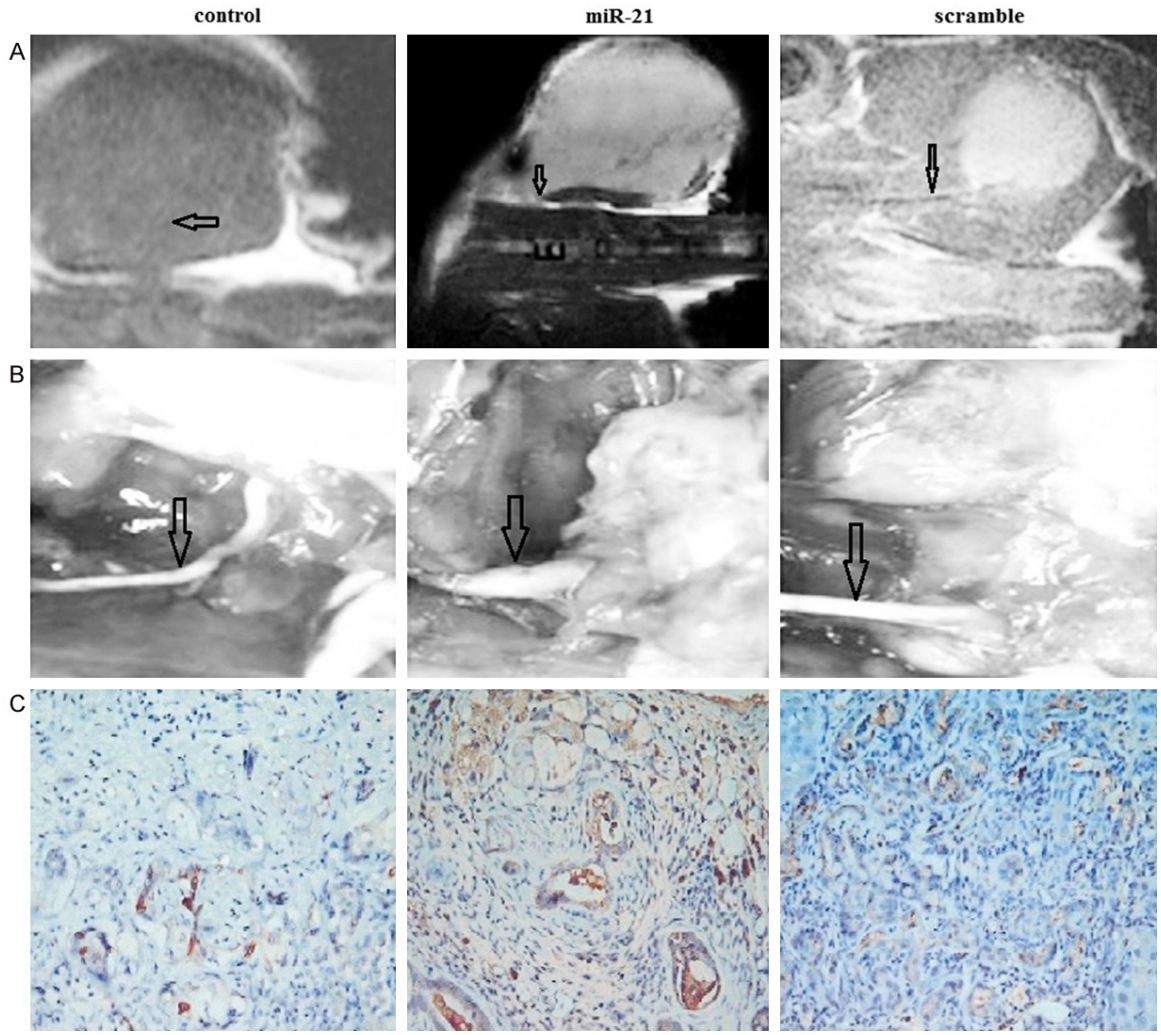

Figure 4. miR-21 facilitates CCLP1 perineural invasion in vivo by magnetic resonance imaging. A. MRI T2 weighted images were taken of mice under anesthesia to visualize the proximal sciatic nerve to assess for PNI. The MRI image of a mouse injected with miR-21/CCLP1 shows a thickened sciatic nerve (arrow) coursing proximal to the injected tumor mass in the sciatic nerve at week 5 after injection. In contrast, the right sciatic nerve of a mouse injected with scramble/CCLP1 demonstrates tumor at the sciatic nerve injection local site, but a nearly normal proximal sciatic nerve caliber (arrow) at week 5 after injection. B. At the time of animal sacrifice, sciatic nerve tumors and the proximal sciatic were surgically exposed. PBS or scramble injected sciatic nerve appears thin and shiny at week 5 after injection. A miR-21/CCLP1 sciatic nerve tumor shows evidence of proximal sciatic nerve invasion and thickening (arrow) consistent with PNI. C. The immunohistochemistry results showing MMP-7 in xenograft tumors formed by implanting miR-21/CCLP1 cells.

involved in PNI, we performed a chemokine screen of explants of murine DRG, which contain primarily neurons and glial cells. DRG explants in Matrigel sprout axonal-like projects which are analogous to tiny nerves, which in co-cultures with cancer cells serve as a model that recapitulates PNI. Our study found that the area of nerve invasion by the miR-21 overexpressing CCLP1 cells was increased by 62% as compared with the scramble transfected CCLP1 cells by day 6 of the co-culture assay. These results demonstrate that miR-21 expression facilitates both CC cell migration and perineural invasion.

We next assessed the contribution of miR-21 in PNI using a murine *in vivo* model of sciatic nerve invasion. The results showed that mice injected with scramble/CCLP1 tumors maintained intact sciatic nerve function over 6 weeks, and miR-21/CCLP1 tumors developed progressive, complete, ipsilateral hind limb pa-

ralysis over 6 weeks. MRI imaging has the same results as above. From the studies above, we suggested that overexpression of miR-21 contributed to cancer PNI.

Previous study has found that miR-21 is involved in the cell migration and tumorigenicity of laryngeal squamous cell carcinoma (LSCC) via the regulation of MMP-7 expression [14]. In the present study, we found that overexpression of miR-21 induced MMP-7 upregulation by western blot and ELISA assay, and targeting MMP-7 inhibited miR-21 induced cell invasion and PNI in vitro. It is suggested that miR-21 targets MMP-7 and promotes perineural invasion of cholangiocarcinoma.

In conclusion, we have demonstrated that miR-21 is significantly upregulated in CC cells. miR-21 overexpression can promote cell migration, invasion and PNI in vitro and in vivo. Furthermore, miR-21 functions at least partially by upregulating MMP-7. Such investigation elucidating these mechanisms may facilitate for the optimal design of future therapeutic strategies intended to disrupt these interactions.

Acknowledgements

This study was supported by grants from Shandong Natural Scientific Research Funds (No: 2014ZRB14302).

Disclosure of conflict of interest

None.

Address correspondence to: Qiang Shen, Department of Imaging, The Affiliated Hospital of Jining Medical College, Jining, China. Tel: +86-1520675-3839; E-mail: shenqiangmri@126.com

References

[1] McGlynn KA, Tarone RE, El-Serag HB. A comparison of trends in the incidence of hepatocellular carcinoma and intrahepatic cholangiocarcinoma in the United States. Cancer Epidemiol Biomarkers Prev 2006; 15: 1198-1203.

[2] Khan SA, Davidson BR, Goldin R, Pereira SP, Rosenberg WM, Taylor-Robinson SD, Thillainayagam AV, Thomas HC, Thursz MR, Wasan H; British Society of Gastroenterology. Guidelines for the diagnosis and treatment of cholangiocarcinoma: consensus document. Gut 2002; 51 Suppl 6: VI1-9.

[3] Murakawa K, Tada M, Takada M, Tamoto E, Shindoh G, Teramoto K, Matsunaga A, Komuro K, Kanai M, Kawakami A, Fujiwara Y, Kobayashi N, Shirata K, Nishimura N, Okushiba S, Kondo S, Hamada J, Katoh H, Yoshiki T, Moriuchi T. Prediction of lymph node metastasis and perineural invasion of biliary tract cancer by selected features from cDNA array data. J Surg Res 2004; 122: 184-194.

[4] Suzuki M, Takahashi T, Ouchi K, Matsuno S. Perineural tumor invasion and its relation with the lymphogenous spread in human and experimental carcinoma of bile duct. A computer-aided 3-D reconstruction study. Tohoku J Exp Med 1994; 172: 17-28.

[5] Kumarswamy R, Volkmann I, Thum T. Regulation and function of miRNA-21 in health and disease. RNA Biol 2011; 8: 706-713.

[6] Zhou L, Yang ZX, Song WJ, Li QJ, Yang F, Wang DS, Zhang N, Dou KF. MicroRNA-21 regulates the migration and invasion of a stem-like population in hepatocellular carcinoma. Int J Oncol 2013; 43: 661-669.

[7] Liu Z, Jin ZY, Liu CH, Xie F, Lin XS, Huang Q. MicroRNA-21 regulates biological behavior by inducing EMT in human cholangiocarcinoma. Int J Clin Exp Pathol 2015; 8: 4684-4694.

[8] Glinsky GV, Krones-Herzig A, Glinskii AB. Malignancy-associated regions of transcriptional activation: gene expression profiling identifies common chromosomal regions of a recurrent transcriptional activation in human prostate, breast, ovarian, and colon cancers. Neoplasia 2003; 5: 218-228.

[9] Miwa S, Miyagawa S, Soeda J, Kawasaki S. Matrix metalloproteinase-7 expression and biologic aggressiveness of cholangiocellular carcinoma. Cancer 2002; 94: 428-434.

[10] Shirabe K, Shimada M, Kajiyama K, Hasegawa H, Gion T, Ikeda Y, Takenaka K, Sugimachi K. Expression of matrix metalloproteinase-9 in surgically resected intrahepatic cholangiocarcinoma. Surgery 1999; 126: 842-846.

[11] Itatsu K, Zen Y, Yamaguchi J, Ohira S, Ishikawa A, Ikeda H, Sato Y, Harada K, Sasaki M, Sasaki M, Sakamoto H, Nagino M, Nimura Y, Ohta T, Nakanuma Y. Expression of matrix metalloproteinase 7 is an unfavorable postoperative prognostic factor in cholangiocarcinoma of the perihilar, hilar, and extrahepatic bile ducts. Hum Pathol 2008; 39: 710-719.

[12] Martin del Campo SE, Latchana N, Levine KM, Grignol VP, Fairchild ET, Jaime-Ramirez AC, Dao TV, Karpa VI, Carson M, Ganju A, Chan AN, Carson WE 3rd. MiR-21 enhances melanoma invasiveness via inhibition of tissue inhibitor of metalloproteinases 3 expression: in vivo effects of MiR-21 inhibitor. PLoS One 2015; 10: e0115919.

[13] Liu LZ, Li C, Chen Q, Jing Y, Carpenter R, Jiang Y, Kung HF, Lai L, Jiang BH. MiR-21 induced angiogenesis through AKT and ERK activation and HIF-1α expression. PLoS One 2011; 6: e19139.
[14] Shen K, Liang Q, Xu K, Cui D, Jiang L, Yin P, Lu Y, Li Q, Liu J. MiR-139 inhibits invasion and metastasis of colorectal cancer by targeting the type I insulin-like growth factor receptor. Biochem Pharmacol 2012; 84: 320-330.
[15] Dong CG, Wu WK, Feng SY, Wang XJ, Shao JF, Qiao J. Co-inhibition of microRNA-10b and microRNA-21 exerts synergistic inhibition on the proliferation and invasion of human glioma cells. Int J Oncol 2012; 41: 1005-1012.
[16] Bakst RL, Lee N, He S, Chernichenko N, Chen CH, Linkov G, Le HC, Koutcher J, Vakiani E, Wong RJ. Radiation impairs perineural invasion by modulating the nerve microenvironment. PLoS One 2012; 7: e39925.
[17] Bapat AA, Hostetter G, Von Hoff DD, Han H. Perineural invasion and associated pain in pancreatic cancer. Nat Rev Cancer 2011; 11: 695-707.
[18] Chatterjee D, Katz MH, Rashid A, Aishima S, Maehara S, Tanaka S. Perineural and intraneural invasion in post-therapy pancreaticoduodenectomy specimens predicts poor prognosis in patients with pancreatic ductal adenocarcinoma. Diagn Mol Pathol 2012; 36: 4 09-417.
[19] Katz B, Srougi M, Dall'oglio M, Nesrallah AJ, Sant'anna AC, Pontes J Jr, Antunes AA, Reis ST, Viana N, Sañudo A, Camara-Lopes LH, Leite KR. Perineural invasion detection in prostate biopsy is related to recurrence-free survival in patients submitted to radical prostatectomy. Urol Oncol 2013; 31: 175-9.
[20] Liebig C, Ayala G, Wilks JA, Berger DH, Albo D. Perineural invasion in cancer: a review of the literature. Cancer 2009; 115: 3379-3391.
[21] Peng J, Sheng W, Huang D, Venook AP, Xu Y, Guan Z, Cai S. Perineural invasion in pT3N0 rectal cancer: the incidence and its prognostic effect. Cancer 2011; 117: 1415-1421.
[22] Solares CA, Lee K, Parmar P, O'Rourke P, Panizza B. Epidemiology of clinical perineural invasion in cutaneous squamous cell carcinoma of the head and neck. Otolaryngol Head Neck Surg 2012; 146: 746-751.
[23] Endo I, Gonen M, Yopp AC, Dalal KM, Zhou Q, Klimstra D, D'Angelica M, DeMatteo RP, Fong Y, Schwartz L, Kemeny N, O'Reilly E, Abou-Alfa GK, Shimada H, Blumgart LH, Jarnagin WR. Intrahepatic cholangiocarcinoma: rising frequency, improved survival, and determinants of outcome after resection. Ann Surg 2008; 248: 84-96.
[24] Fisher SB, Patel SH, Kooby DA, Weber S, Bloomston M, Cho C, Hatzaras I, Schmidt C, Winslow E, Staley CA 3rd, Maithel SK. Lymphovascular and perineural invasion as selection criteria for adjuvant therapy in intrahepatic-cholangiocarcinoma: a multi-institution analysis. HPB (Oxford) 2012; 14: 514-522.
[25] Liebig C, Ayala G, Wilks JA, Berger DH, Albo D. Perineural invasion in cancer: a review of the literature. Cancer 2009; 115: 3379-3391.
[26] Sousa LO, Sobral LM, Matsumoto CS, Saggioro FP, López RV, Panepucci RA, Curti C, Silva WA Jr, Greene LJ, Leopoldino AM. Lymph node or perineural invasion is associated with low miR-15a, miR-34c and miR-199b levels in head and neck squamous cell carcinoma. BBA Clin 2016; 6: 159-164.
[27] Prueitt RL, Yi M, Hudson RS, Wallace TA, Howe TM, Yfantis HG, Lee DH, Stephens RM, Liu CG, Calin GA, Croce CM, Ambs S. Expression of microRNAs and protein-coding genes associated with perineural invasion in prostate cancer. Prostate 2008; 68: 1152-64.